Notes

Synthesis and Characterization of a Novel Asymmetric Ferrocene Alkoxycarboxylate of Titanium, $Ti_4O_2(O^iPr)_6\{(\eta^5\text{-}O_2CC_5H_4)Fe(\eta^5\text{-}C_5H_5)\}_6$

Alec Bailey, Maoyu Shang, and Thomas P. Fehlner*

Department of Chemistry and Biochemistry,
251 Nieuwland Science Hall, University of Notre Dame,
Notre Dame, Indiana 46556

Received July 17, 2000

Introduction

The use of organic carboxylic acids to modify the reactivity of titanium alkoxides has led to the isolation of a variety of complex molecules containing titanium oxyalkoxide cores coordinated by carboxylate ligands.[1−6] We have shown that a transition metal cluster carboxylic acid used in place of an organic acid generates strikingly different cores.[7−9] In addition, while the reaction with organic acids is rather sensitive to factors such as the alkyl or aryl group of the alkoxide as well as stoichiometry, the reaction with the cluster acid is much less so. Thus, reaction of $(CO)_9Co_3CCO_2H$ with $Ti(OR)_4$ yields $Ti_4O_4(OR)_4\{(CO)_9Co_3CCO_2\}_4$ with a Ti_4O_4 cubanelike core for a variety of alkyl and aryl R groups.[8] Apparently, the steric bulk and/or the electronic effect of the metal cluster has a more dominating effect on the condensation reaction than a purely organic substituent.

We were interested in exploring the ramifications of this observation for two reasons. First, $Ti_4O_4(OR)_4\{(CO)_9Co_3CCO_2\}_4$ exhibits a nearly square array of clusters and offers some potential as a redox-active cluster square for use in molecular electronics.[10] However, the reduction properties of the tricobalt cluster are sensitive to the alkyne substitutent[11] and a more robust redox center is desirable. Second, the factors that drive the condensation chemistry are not clear. The use of a mononuclear compound of somewhat smaller bulk provides a significant test; i.e., will the cubane core be produced or something else? Metal ferrocene carboxylates have been reported by others,[12] and we have now investigated the reaction of $\{(\eta^5\text{-}C_5H_5)Fe(\eta^5\text{-}C_5H_4COOH)\}$ with $Ti(O^iPr)$, ^{i}Pr = isopropyl. Here we report the isolation of a titanium oxyalkoxide core of unprecedented structure that supports an asymmetric array of coordinated ferrocene carboxylate ligands.

Experimental Section

$Ti_4O_2(O^iPr)_6\{(\eta^5\text{-}O_2CC_5H_4)Fe(\eta^5\text{-}C_5H_5)\}_6$. Standard air- and water-free techniques were employed, and starting materials (Aldrich) were used as received. A 250 mL round-bottom Schlenk flask equipped with a magnetic stir bar was flushed with dinitrogen for 5 min and charged with 0.460 g (2 mmol) of $(\eta^5\text{-}C_5H_5)Fe(\eta^5\text{-}C_5H_4COOH)$. Freshly distilled THF (∼25 mL) was added, and the resulting mixture was stirred for several minutes to dissolve the carboxylic acid. To this solution 0.34 mL (0.327 g, 1.15 mmol) of $Ti(OiPr)_4$ was added via syringe. Addition of the alkoxide produces a dark-red coloration that disappears with prolonged stirring. After complete addition of $Ti(OiPr)_4$, the mixture was stirred for an additional 30 min before being heated to 50 °C. The solution was maintained at this temperature for 3 h and then cooled to room temperature. The solvent was removed in vacuo, leaving an orange solid in the flask. To this solid, 20 mL of freshly distilled hexanes was added. The solution was filtered through a funnel with a 2 cm Celite layer. The filtrate was reduced to approximately 10 mL and placed in a refrigerator after which 469 mg of crystalline orange solid (60% yield based on total mass) was recovered.

Spectroscopic Characterization. ^{1}H NMR ($CDCl_3$, δ, ppm): 4.93 (m, $C_5H_4CO_2$), 4.70 (sept, $-CH(CH_3)_2$), 4.41 (m, $C_5H_4CO_2$), 4.30 (s, Cp ring), 4.01 (sept, $-CH(CH_3)_2$), 1.42 (d, $-CH(CH_3)_2$), 1.20 (d, $-CH(CH_3)_2$). ^{13}C ($CDCl_3$, δ, ppm): 180.5 ($-CO_2$), 79.0 ($-CH(CH_3)_2$), 71.0 ($C_5H_4CO_2$), 70.3 ($C_5H_4CO_2$), 69.4 (Cp), 63.7 ($-CH(CH_3)_2$), 24.7 ($-CH(CH_3)_2$), 24.5 ($-CH(CH_3)_2$). FTIR (KBr, cm^{-1}): 1577 m, 1523 m, 1483 s, 1398 s, 1362 s, 1349 m (sh), 1198 m, 1164 m, 1129 m, 1106 m, 1022 m, 1003 m, 818 m, 722 s, 520 s, 480 m.

XRD Characterization. A concentrated solution (CH_2Cl_2) was layered with a 1:1 mixture of CH_2Cl_2 and Et_2O followed by a layer of Et_2O in a 100 mL Schlenk tube. The Schlenk tube was placed in a refrigerator. Several days later two types of crystals were observed on the tube walls: orange plates and red blocks. Both types of crystals were investigated by single-crystal X-ray diffraction, but only the former yielded a result.

An orange platelike crystal with a refined effective mosaic spread of 0.524 was sealed for data collection on an Enraf-Nonius FAST area detector diffractometer operating at 130 K. A summary of the parameters is given in Table 1. All reflections were reduced using Lorentz polarization factors. The structure was solved by direct methods using SHELXS-86. Most of the non-hydrogen atoms were shown on an E map. Ensuing least-squares refinement and difference Fourier synthesis showed the rest of the non-hydrogen atoms and also two dichloromethane solvent molecules with partial occupancy coefficients. After all these non-hydrogen atoms were refined anisotropically, most of the hydrogen atoms were shown on a difference Fourier map. However, in the final refinement, hydrogen atoms were restrained by using riding models. Apart from averaging large numbers of equivalent and redundant reflections collected at different diffractometer settings, a modified DIFABS program DIFFAST was used to further alleviate the influence of absorption. The structure was refined against F^2 by the SHELXL-93 program. The refinement converged, and the weighted R factors, wR, are based on F^2, and conventional R factors, R, are based on F, with F set to zero for negative intensities. All reflections, including

(1) Doeuff, S.; Dromzee, Y.; Taulelle, F.; Sanchez, C. *Inorg. Chem.* **1989**, *28*, 4439.
(2) Doeuff, S.; Dromzee, Y.; Sanchez, C. *C. R. Acad. Sci. Paris, Ser. II* **1989**, *308*, 1409.
(3) Boyle, T. J.; Tafoya, C. J.; Scott, B. In National ACS Meeting, New Orleans, LA, 1996; Abstract O62.
(4) Boyle, T. J.; Tyner, R. P.; Alam, T. M.; Scott, B. L.; Ziller, J. W.; Potter, B. G. J. *J. Am. Chem. Soc.* **1999**, *121*, 12104.
(5) Gautier-Luneau, I.; Mosset, A.; Galy, J. *Z. Kristallogr.* **1987**, *180*, 83.
(6) Toledano, P.; In, M.; Sanchez, C. C. *C. R. Acad. Sci. Paris, Ser. II* **1991**, *313*, 1247.
(7) Lei, X.; Shang, M.; Fehlner, T. P. *Organometallics* **1996**, *15*, 3779.
(8) Lei, X.; Shang, M.; Fehlner, T. P. *Organometallics* **1997**, *16*, 5289.
(9) Shimomura, H.; Lei, X.; Shang, M.; Fehlner, T. P. *Organometallics* **1997**, *16*, 5302.
(10) Lent, C. S. *Science* **2000**, *288*, 1597.
(11) Peake, B. M.; Robinson, B. H.; Simpson, J.; Watson, D. J. *Inorg. Chem.* **1977**, *16*, 405.
(12) Churchill, M. R.; Li, Y.-J.; Nalewajek, D.; Schaber, P. M.; Dorfman, J. *Inorg. Chem.* **1985**, *24*, 2684.

10.1021/ic000790d CCC: $19.00
Published on Web 08/30/2000

Table 1. Crystal Data and Structure Refinement for $Ti_4O_2(OiPr)_6(O_2CCpFeCp)_6 \cdot 1.32CH_2Cl_2$

empirical formula	C85.32 H98.64 Cl2.64 Fe6 O20 Ti4
fw	2064.41
cryst syst	monoclinic
space group	$P2_1/c$
a, Å	17.090(5)
b, Å	21.612(4)
c, Å	24.548(5)
β, deg	100.129(14)
volume, Å^3	8925(4)
Z	4
density (calcd), Mg/m^3	1.536
F(000)	4238
wavelength, Å	0.710 73
abs coeff, mm^{-1}	1.428
cryst size	0.30 mm × 0.10 mm × 0.07 mm
temp, K	130(2) K
diffractometer	Enraf-Nonius FAST
θ range for data collection, deg	2.24−30.08
index ranges	$-14 \le h \le 23$, $-26 \le k \le 30$, $-34 \le l \le 34$
total data collected	66 181
unique data	23 903 [$R_{int} = 0.0808$]
refinement method	full-matrix on F^2 (SHELXL-93)
data/restraints/parameters	23903/10/1084
goodness-of-fit on F^2	1.016
final *R* indices [$I > 2\sigma(I)$]	R1 = 0.0693, wR2 = 0.1549
R indices (all data)	R1 = 0.1124, wR2 = 0.1785
largest diffraction peak and hole	1.657 and −1.443 e/Å^3

Table 2. Selected Bond Distances (Å) for $Ti_4O_2(OiPr)_6(O_2CCpFeCp)_6 \cdot 1.32CH_2Cl_2$

Ti(1)−O(4)	1.769(3)	Ti(3)−O(1)	1.913(3)
Ti(1)−O(3)	1.803(3)	Ti(3)−O(14)	2.005(3)
Ti(1)−O(9)	2.022(3)	Ti(3)−O(18)	2.055(3)
Ti(1)−O(13)	2.058(3)	Ti(3)−O(16)	2.088(3)
Ti(1)−O(1)	2.062(3)	Ti(3)−Ti(4)	2.8953(11)
Ti(1)−O(11)	2.064(3)	Ti(4)−O(8)	1.777(3)
Ti(2)−O(6)	1.781(3)	Ti(4)−O(1)	1.914(3)
Ti(2)−O(5)	1.805(3)	Ti(4)−O(2)	1.916(3)
Ti(2)−O(15)	2.019(3)	Ti(4)−O(20)	2.008(3)
Ti(2)−O(2)	2.048(3)	Ti(4)−O(10)	2.054(3)
Ti(2)−O(19)	2.063(3)	Ti(4)−O(12)	2.073(3)
Ti(2)−O(17)	2.101(3)	O(3)−C(1)	1.418(6)
Ti(3)−O(7)	1.784(3)	C(1)−C(3)	1.492(8)
Ti(3)−O(2)	1.911(3)		

those with negative intensities, were included in the refinement. The highest residual electron density was around the solvent molecules, which was indicative of a disorder. However, attempts to model the disorder failed to give any positive result. Selected bond distances and angles are given in Tables 2 and 3, respectively.

Results and Discussion

The structure of $Ti_4O_2(O^iPr)_6\{(\eta^5\text{-}O_2CC_5H_4)Fe(\eta^5\text{-}C_5H_5)\}_6$ (Figures 1−3) exhibits bridging ferrocene carboxylate, terminal alkoxide, and μ^3-bridging oxide ligands. As expected, each titanium atom is located at the center of an approximately octahedral array of oxygen atoms. There are two types of titanium atoms: one with two oxo, three carboxylate, and one alkoxide oxygen atom nearest neighbors and one with one oxo, three carboxylate, and two alkoxide oxygen atom neighbors (Figure 1). The core can be related to the cube shown in Figure 4a, the core found in $Ti_4O_4(OR)_4\{(CO)_9Co_3CCO_2\}_4$.[8] Figure 4b shows a dual corner-missing cube, several examples of which were reported recently by Boyle et al.[4] The core of the new compound is also a dual corner-missing cube; however, the corners missing are nonadjacent oxides. In addition the two titanium atoms coordinated to a single oxide ligand are bent outward, generating a quasi-planar Ti_4O_2 fragment (Figures 1 and 4c). The bond distances Ti(3)−O(1) = 1.913(3) Å, Ti(3)−O(2) = 1.911(3) Å, Ti(4)−O(1) = 1.914(3) Å, and Ti(4)−O(2) = 1.916(3) Å are shorter than Ti(1)−O(1) = 2.062(3) Å and Ti(2)−O(2) = 2.048(3) Å. The Ti(3)−Ti(4) distance (2.8953(11) Å) is typical of that found in the cubes described earlier.

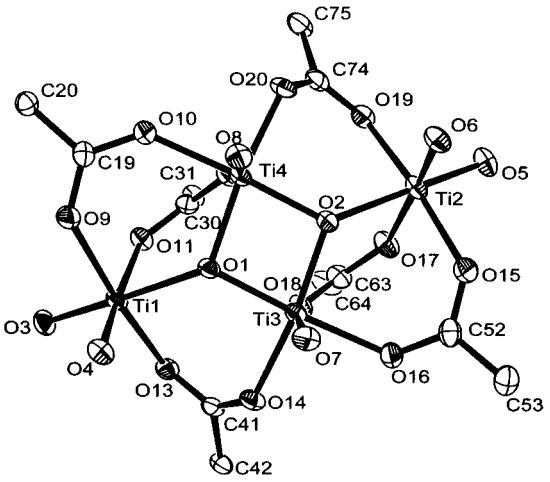

Figure 1. Core of $Ti_4O_2(O^iPr)_6(O_2CCpFeCp)_6$. Thermal ellipsoids shown at 20% probability. Ferrocene moietes, except for the ipso carbons, and isopropyl groups are omitted for clarity.

Table 3. Selected Bond Angles (deg) for $Ti_4O_2(OiPr)_6(O_2CCpFeCp)_6 \cdot 1.32CH_2Cl_2$

O(4)−Ti(1)−O(3)	97.81(14)	O(7)−Ti(3)−O(18)	165.30(13)
O(4)−Ti(1)−O(9)	93.12(13)	O(2)−Ti(3)−O(18)	86.39(11)
O(3)−Ti(1)−O(9)	92.27(13)	O(1)−Ti(3)−O(18)	93.50(12)
O(4)−Ti(1)−O(13)	96.76(13)	O(14)−Ti(3)−O(18)	80.34(11)
O(3)−Ti(1)−O(13)	86.89(12)	O(7)−Ti(3)−O(16)	85.33(13)
O(9)−Ti(1)−O(13)	170.10(12)	O(2)−Ti(3)−O(16)	94.97(12)
O(4)−Ti(1)−O(1)	91.03(13)	O(1)−Ti(3)−O(16)	174.26(12)
O(3)−Ti(1)−O(1)	170.50(13)	O(14)−Ti(3)−O(16)	90.36(12)
O(9)−Ti(1)−O(1)	90.71(11)	O(18)−Ti(3)−O(16)	81.65(12)
O(13)−Ti(1)−O(1)	88.62(11)	O(7)−Ti(3)−Ti(4)	101.57(10)
O(4)−Ti(1)−O(11)	173.73(12)	O(2)−Ti(3)−Ti(4)	40.90(9)
O(3)−Ti(1)−O(11)	88.32(13)	O(1)−Ti(3)−Ti(4)	40.84(8)
O(9)−Ti(1)−O(11)	85.29(12)	O(14)−Ti(3)−Ti(4)	131.97(9)
O(13)−Ti(1)−O(11)	84.83(12)	O(18)−Ti(3)−Ti(4)	92.55(9)
O(1)−Ti(1)−O(11)	82.94(11)	O(16)−Ti(3)−Ti(4)	135.87(9)
O(6)−Ti(2)−O(5)	98.08(14)	O(8)−Ti(4)−O(1)	102.22(13)
O(6)−Ti(2)−O(15)	90.76(14)	O(8)−Ti(4)−O(2)	99.66(13)
O(5)−Ti(2)−O(15)	94.37(14)	O(1)−Ti(4)−O(2)	81.46(12)
O(6)−Ti(2)−O(2)	91.37(12)	O(8)−Ti(4)−O(20)	93.31(13)
O(5)−Ti(2)−O(2)	169.67(13)	O(1)−Ti(4)−O(20)	163.64(12)
O(15)−Ti(2)−O(2)	89.64(12)	O(2)−Ti(4)−O(20)	91.01(12)
O(6)−Ti(2)−O(19)	97.85(13)	O(8)−Ti(4)−O(10)	85.81(13)
O(5)−Ti(2)−O(19)	86.29(14)	O(1)−Ti(4)−O(10)	95.17(12)
O(15)−Ti(2)−O(19)	171.19(12)	O(2)−Ti(4)−O(10)	174.05(12)
O(2)−Ti(2)−O(19)	88.30(12)	O(20)−Ti(4)−O(10)	90.99(12)
O(6)−Ti(2)−O(17)	174.06(13)	O(8)−Ti(4)−O(12)	165.11(13)
O(5)−Ti(2)−O(17)	87.79(13)	O(1)−Ti(4)−O(12)	86.39(11)
O(15)−Ti(2)−O(17)	87.84(12)	O(2)−Ti(4)−O(12)	93.57(12)
O(2)−Ti(2)−O(17)	82.85(11)	O(20)−Ti(4)−O(12)	79.58(11)
O(19)−Ti(2)−O(17)	83.40(12)	O(10)−Ti(4)−O(12)	81.29(12)
O(7)−Ti(3)−O(2)	101.59(12)	O(8)−Ti(4)−Ti(3)	101.87(10)
O(7)−Ti(3)−O(1)	99.83(13)	O(1)−Ti(4)−Ti(3)	40.84(9)
O(2)−Ti(3)−O(1)	81.60(12)	O(2)−Ti(4)−Ti(3)	40.76(8)
O(7)−Ti(3)−O(14)	92.98(12)	O(20)−Ti(4)−Ti(3)	130.93(9)
O(2)−Ti(3)−O(14)	164.83(12)	O(10)−Ti(4)−Ti(3)	136.00(8)
O(1)−Ti(3)−O(14)	91.85(12)	O(12)−Ti(4)−Ti(3)	92.59(8)

Each ferrocene carboxylate bridges two titanium centers, placing four of the ferrocene moieties on the periphery of the core to form an approximately square array when viewed from above or below the Ti_4O_2 curved surface (Figure 2). The arrangement of alkoxide and ferrocene carboxylate ligands results in a single C_2 axis perpendicular to a line joining the

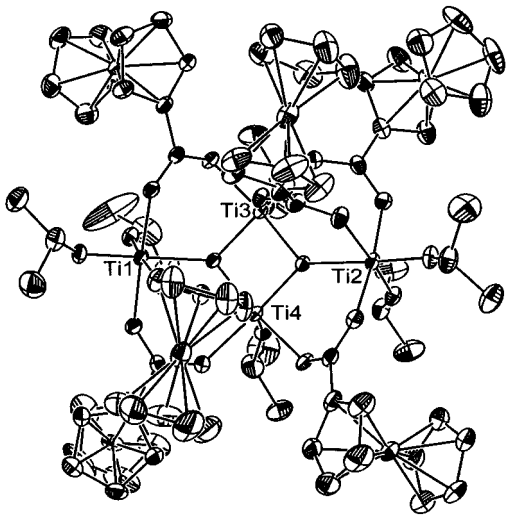

Figure 2. Top view of $Ti_4O_2(O^iPr)_6(O_2CCpFeCp)_6$. Hydrogen atoms are omitted for clarity.

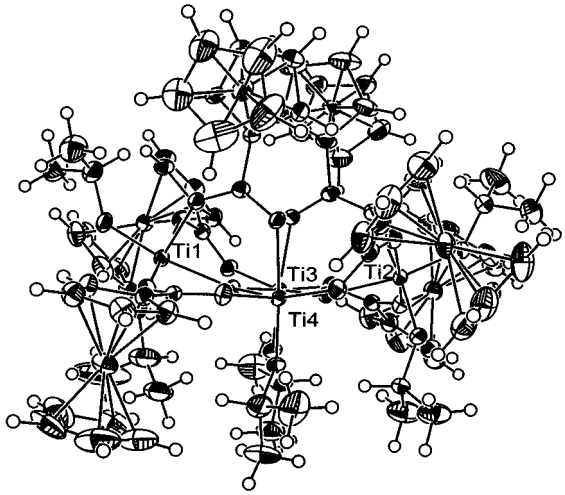

Figure 3. Side view of $Ti_4O_2(O^iPr)_6(O_2CCpFeCp)_6$ including hydrogen atom positions. The alkoxide side lies toward the bottom of the figure and the ferrocene side toward the top.

Ti(3)−Ti(4) atoms (Figure 4c). On the concave side of the Ti_4O_2 surface are found two bridging ferrocene carboxylates and two terminal isopropoxide ligands, whereas the convex side exhibits only four terminal isopropoxide ligands (Figure 3). Thus, the molecule possesses two distinctly different sides—one alkoxide and one mixed alkoxide/ferrocene.

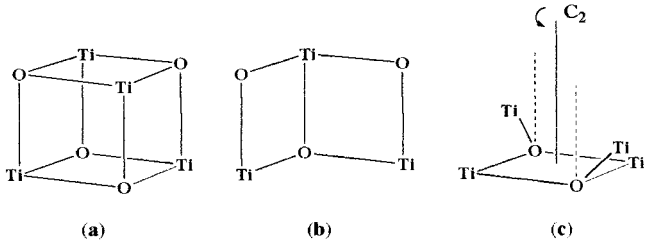

Figure 4. Relationship of (a) cubane core to (b) adjacent dual corner-missing cube and (c) nonadjacent dual corner-missing cube.

The ^1H and ^{13}C NMR spectra suggest higher symmetry than expected on the basis of the solid-state structure. Only two types of isopropoxide groups are observed and only one type of ferrocene carboxylate. (The cyclopentadienyl protons also integrate low, but this is not uncommon.) Several explanations are possible including fluxional behavior and structural rearrangement. However, degradation accompanied by the formation of soluble fragments can be ruled out.

Because the redox behavior of these metal arrays are of interest to us relative to our interests in molecular electronics, we briefly investigated the cyclic voltammetry behavior of $Ti_4O_2(O^iPr)_6\{(\eta^5\text{-}O_2CC_5H_4)Fe(\eta^5\text{-}C_5H_5)\}_6$. Unfortunately, the oxidation associated with the ferrocene units is irreversible and this particular compound is not a useful one for the contemplated application.

Conclusions

Previously we associated the 1:1 ratio of Ti to cluster ligand in the cluster carboxylate possessing a cubane core with its generation from a $Ti(OR)_3\{(CO)_9Co_3CCO_2\}$ intermediate.[8] Slow addition of another $(CO)_9Co_3CCO_2H$ to the intermediate relative to formation of $Ti_4O_4(OR)_4\{(CO)_9Co_3CCO_2\}_4$ is consistent with observed product stoichiometry. This new work confirms that the metal species plays an active role. The change of the $-CCo_3(CO)_9$ fragment to ferrocene for the same alkoxide generates a different central titanium oxyalkoxide core that also differs from those generated from organic acids.

Acknowledgment. This work has been supported by ONR/DARPA under the Moletronics program N00014-99-1-0472.

Supporting Information Available: Crystallographic files in CIF format. This material is available free of charge via the Internet at http://pubs.acs.org.

IC000790D